



Obrabotka metallov -

Metal Working and Material Science

Journal homepage: http://journals.nstu.ru/obrabotka_metallov







Structural features and tribological properties of multilayer high-temperature plasma coatings





Natalia Pugacheva^{1, 2, a}, Tatyana Bykova^{1, 2, b, *}, Vitaly Sirosh^{3, c}, Alexey Makarov^{3, d}

¹ Institute of Engineering Science Ural Branch, Russian Academy of Sciences, 34 Komsomolskaya str., Yekaterinburg, 620049, Russian Federation

² Ural Federal University named after the first President of Russia B.N. Yeltsin, 19 Mira str., Ekaterinburg, 620002, Russian Federation

³ M.N. Miheev Institute of Metal Physics, Ural Branch of the Russian Academy of Sciences, 18 S. Kovalevskoy str., Ekaterinburg, 620108, Russian Federation

^a  <https://orcid.org/0000-0001-8015-8120>,  nata5-4@yandex.ru; ^b  <https://orcid.org/0000-0002-8888-6410>,  tatiana_8801@mail.ru;

^c  <https://orcid.org/0000-0002-8180-9543>,  sirosh.imp@yandex.ru; ^d  <https://orcid.org/0000-0002-2228-0643>,  av-mak@yandex.ru

ARTICLE INFO

Article history:

Received: 31 May 2024

Revised: 22 June 2024

Accepted: 08 July 2024

Available online: 15 September 2024

Keywords:

Plasma spraying
 Multilayer coating
 Iron oxide
 Strengthening phases
 Micromechanical properties
 Friction coefficient
 Wear resistance

Funding

The work was carried out within the framework of the state assignment of the IMASH Ural Branch of the Russian Academy of Sciences on topic No. 124020700063-3 on the equipment of the Center for Shared Use "Plastometry".

The work was carried out within the framework of the state assignment of the Institute of Physics and Mathematics, Ural Branch of the Russian Academy of Sciences on the topic "Structure" No. 122021000033-2.

ABSTRACT

Introduction. Multilayer high-temperature coatings obtained using plasma spraying, are studied. The combination of layers of different chemical and phase compositions made it possible to increase wear resistance by 1.5–2.0 times. **The purpose of this work** is to study the influence of the chemical composition of sprayed coatings on the phase composition, structure, micromechanical and tribological characteristics under conditions of dry sliding friction of surface layers. **Materials and methods of research.** Coatings A and B consist of sequentially sprayed layers. The first and second layers were sprayed in a reducing atmosphere: the *first layer* was a heat-resistant self-fluxing powder of two systems: 1 – Fe-Cr-Si-Mn-B-C for coating A and 2 – Fe-Ni-Si-Mn-B-C for coating B; the *second layer* was a mixture of self-fluxing powder with iron powder in a 1:1 ratio. The *third layer* was obtained by spraying iron powder in an oxidizing atmosphere to form a metal oxide coating. To create a layer of scale on the surface, coated specimens were subjected to high-temperature annealing at a temperature of 1,000 °C. The chemical composition and nature of the distribution of elements over the thickness of the coatings were determined by micro-X-ray spectral analysis using a *TWSCAN* scanning electron microscope with an *Oxford* energy-dispersive attachment. Microhardness and micromechanical properties were studied using an instrumental microhardness tester of the *Fischerscope HM2000 XYm* system at a load of 0.980 N. Determination of tribological properties was carried out on a laboratory installation using the "finger-disc" scheme at loads of 30, 75, 100 and 130 N. To measure roughness parameters and obtain 3-D profilometry of surfaces after testing, a non-contact profilometer-profiler Optical profiling system *Veeco WYKO NT 1100* was used. **Results and discussion.** Metallographic studies have shown that the formed multilayer coatings consist of an internal metal layer and an external oxide layer with a total thickness of the entire coating up to 800–850 µm. It is established that the first sprayed layer has the highest level of microhardness, which is due to the high-volume fraction of the strengthening phases contained in it (~ 95 %). It is shown that the coating A has increased wear resistance, which is expressed by minimal weight loss (~ 1.5 times less than that of the coating of the coating B), the friction coefficient was $f = 0.3$ for coating A and $f = 0.4$ for coating B. The study of wear surfaces has shown that for all selected test loads under sliding friction conditions, the coating of both compositions was preserved, even at a maximum load of 130 N.

For citation: Pugacheva N.B., Bykova T.M., Sirosh V.A., Makarov A.V. Structural features and tribological properties of multilayer high-temperature plasma coatings. *Obrabotka metallov (tekhnologiya, oborudovanie, instrumenty) = Metal Working and Material Science*, 2024, vol. 26, no. 3, pp. 250–266. DOI: 10.17212/1994-6309-2024-26.3-250-266. (In Russian).

Introduction

Increasing the durability of high-temperature multilayer coatings for parts operating in wear conditions at high operating temperatures in various industrial areas is a relevant objective for the following reasons: firstly, the resulting coatings should have high temperature and oxidation resistance; secondly, it should retain adhesion to the base material; thirdly, it should have high corrosion resistance [1]. The choice of

* Corresponding author

Bykova Tatiana M., Ph.D. (Engineering), Senior Researcher
 Institute of Engineering Science Ural UB RAS,
 34 Komsomolskaya str.,
 620049, Yekaterinburg, Russian Federation
 Tel.: +7 343 362-30-43, e-mail: tatiana_8801@mail.ru

the composition of coatings and the method of its formation on the surface of the part is determined by the operating conditions, which leads to the need for an individual approach to the formation of multilayer coatings of different chemical composition [2–3].

The application of multilayer high-temperature coatings for piercing tools in the production of seamless hot-rolled steel pipes, which are used as structural pipes in construction, mechanical engineering, and oil industry, is promising [4]. The piercing mandrel is used in the production of hollow billets, from which a seamless pipe is produced in subsequent rolling, rolling, reducing, straightening and calibrating mills [5]. The mandrel is exposed to both high temperatures and abrasive wear during operation [6, 7]. To improve the strength and wear resistance, as well as to avoid sticking on the mandrel, its surface is subjected to hardening treatment, by applying a protective high-temperature coating on its toe and spherical surface, followed by an oxidized layer on the outer surface of the material.

To form high-temperature coatings resistant to abrasive wear at high sliding speeds, various self-fluxing high and medium-carbon iron-based alloys alloyed with chromium, nickel, vanadium and manganese are used [8–10]. Iron powder is used to form an oxidized layer on the outer surface, which is applied in an oxidizing atmosphere. Applying an oxide outer layer has a number of advantages: firstly, the oxide layer prevents material from sticking to the mandrel during operation; secondly, at high operating temperatures it creates additional thermal resistance, increasing the thermal resistance of the coating itself; thirdly, at high operating temperatures, scale softens, and it begins to work as a lubricant with the contacted surface [11–15].

Thus, the **purpose of the work** is to study the influence of the chemical composition of sprayed coatings on the phase composition, structure, micromechanical and tribological characteristics under conditions of dry sliding friction of surface layers.

Materials and research methods

In this work, multilayer coatings of two different compositions consisting of three successively applied layers were investigated. The difference in the composition of the obtained coatings is the first layer, for the formation of which heat-resistant self-fluxing iron-based powders were used (Table 1). To obtain the first layer of coating of composition 1, *Fe-Cr-Si-Mn-B-C* powder with a particle size of 50–90 µm was used (Fig. 1 *a*). The first coating layer of composition 2 is *Fe-Ni-Si-Mn-B-C* powder with a particle size of 60–100 µm (Fig. 1 *b*). A mixture of *Fe* powder with self-fluxing powder in ratio (1:1) was used to form the second layer of both coatings and the third layer was obtained from *Fe* powder with particle size of 40–100 µm (Fig. 1 *c*).

All layers of the studied coatings were obtained by plasma-powder spraying technology with contact excitation of arc discharge *UPN-60KM TSP2017*, manufacturer LLC “NPP TSP” (Ekaterinburg).

The first (metal) layer, which chemical composition shown in Table 1, due to its high hardness and wear resistance protects the mandrel material from destruction in case of wear of the upper layers during operation. The second (transition) layer is obtained by spraying a mixture of self-fluxing powder with *Fe* powder. It is designed for a smooth change of properties as well as for better adhesion of the outer layer to

Table 1

Composition of sprayed powders

Powder	Content of chemical elements, mass. %						
	<i>Ni</i>	<i>Cr</i>	<i>Si</i>	B	C	Mn	Fe
Composition 1 (powder <i>Fe-Cr-Si-Mn-B-C</i>)	–	3.8	2.3	3.6	1.2	1.0	base
Composition 2 (powder <i>Fe-Ni-Si-Mn-B-C</i>)	9.0	–	1.2	2.7	0.5	4.0	base

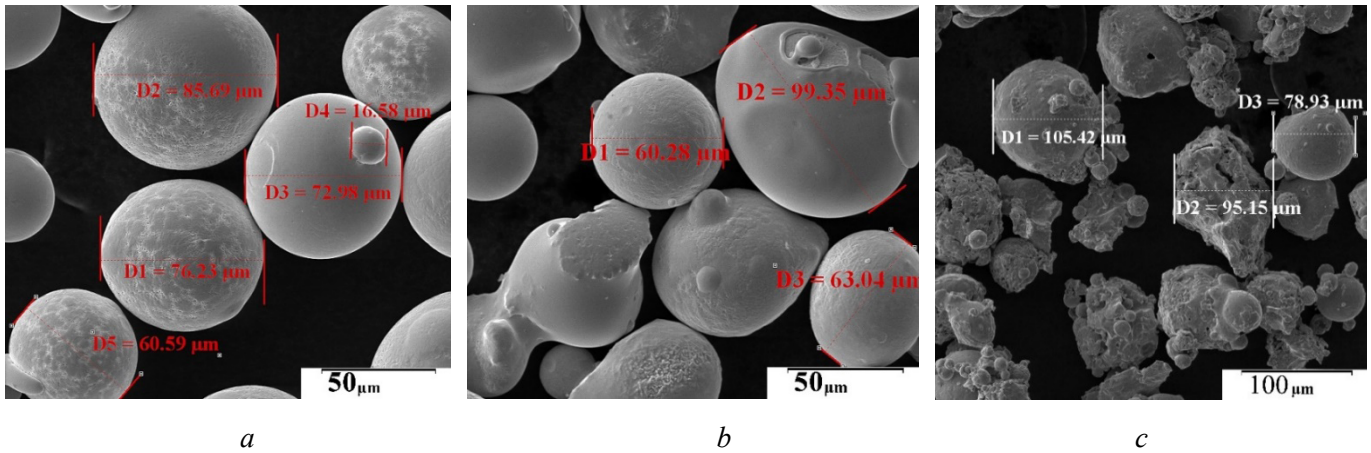


Fig. 1. Morphology of powder particles for obtaining a multilayer coating:
a – powder of composition 1; b – powder of composition 2; c – Fe powder

the inner layer. In order to create a surface scale layer, and to equalize the chemical composition of all layers and increase its adhesion, the coated specimens were subjected to high-temperature annealing at 1,000 °C. The coating containing the first layer with chromium (composition 1 in Table 1) will be conventionally designated as coating *A*, and the coating with nickel-containing inner layer (composition 2 in Table 1) will be conventionally designated as coating *B*.

Microstructure, chemical composition, structure features and thickness of the obtained coatings were studied on cross cuts by means of a *TESCAN VEGAII XMU* scanning electron microscope with an energy dispersive attachment of *OXFORD HKL NordlysF+* at 100 to 800-fold magnification.

By the microindentation method, using a *Fischerscope HM2000 XYm* measuring system with a *Vickers* indenter and *WIN-HCU* software at a maximum load of 0.980 N, the characteristics that reflect the features of the mechanical behavior of the studied coatings under elastic-plastic deformation were determined [16]. Strength indices (microhardness *HV*, *H_{IT}*, *HM* and contact modulus of elasticity (*E**)) and plasticity indices (elastic recovery (*Re*), work of plastic deformation (*φ*) and creep (*CIT*) during indentation) were determined. The values of *Re*, *φ* and *CIT* were calculated according to the formulas:

$$Re = \frac{h_{\max} - h_p}{h_{\max}} \cdot 100\%; \quad (1)$$

$$\varphi = \left(1 - \frac{We}{Wt}\right) \cdot 100\%; \quad (2)$$

$$CIT = \frac{h_{\max} - h_l}{h_l} \cdot 100\%. \quad (3)$$

where *We* is a work of elastic deformation during indentation, released at removal of the applied load; *Wt* is a total mechanical work during indentation; *h_l* is a depth of indenter insertion; *h_{max}* is a maximum depth of indenter insertion.

Investigation of tribological properties was carried out on a laboratory setup using the “pin-on-disc” scheme according to Fig. 2. The friction speed was 5 m/s at loads of 30, 75, 100 and 130 N. In each test, the sliding distance was 5,000 m. The “pin” specimens were made of *A*-coated and *B*-coated steel. The “disc” specimen was a disc made of 12 *Cr-Mo* steel. The tests measured the friction force using a leaf spring with resistance strain gauges glued on it. The heating of the friction surfaces occurred due to the friction itself; external heating sources were not used. The heating temperature of the friction surface was measured using a thermocouple mounted on a “pin” specimen near the friction surface.

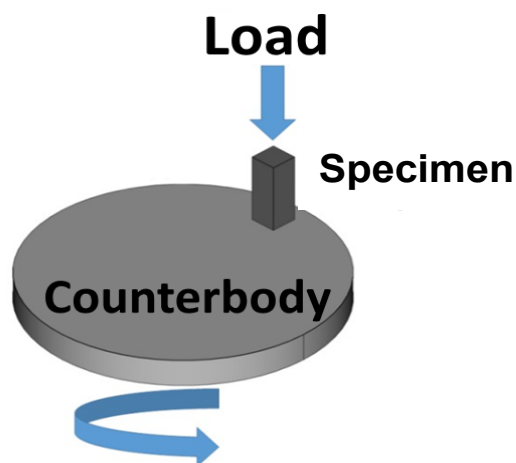


Fig. 2. Tribological loading scheme “pin-on-disc”

To measure the roughness parameters and obtain 3-D profilometry of the surfaces of the coated specimens in the initial state and after testing, a non-contact profilometer-profilograph *Optical profiling system Veeco WYKO NT 1100* was used.

Results and discussion

Determination of the structure and phase composition of coatings

The results of metallographic studies showed that the formed multilayer coatings consist of sequentially applied layers with the total thickness of the entire coating up to 800–850 μm . Figure 3 shows the microstructure and distribution of elements in the obtained coatings. Previously performed phase X-ray diffraction analysis [17] showed that the first (metal) layer of coating **A** of composition **1** (denoted by number **1** in Fig. 3 *a*) consists of a solid solution of *Cr*, *Si* and *Mn* in $\alpha\text{-Fe}$ with strengthening phases in the form of carbides and silicides of chromium and manganese (Cr_{23}C_6 , Cr_5Si_3 , CrSi , Cr_3Si and Mn_5Si_3) and iron borides FeB (Fe_2B). The metal layer of coating **B** of composition **2** (denoted by number **1** in Fig. 3 *b*) consists of two solid solutions of ferrite ($\alpha\text{-Fe}$) and austenite ($\gamma\text{-Fe}$). The strengthening phases are dispersion carbides, silicides and borides (NiSi_2 , Ni_3Si_2 , Mn_5Si_3 , Fe_5Si_3 , Fe_2B). The second (transition) layer and the outer (oxide) layer (denoted by numbers **2** and **3** in Fig. 3 *a* and *b*) on both coatings consist of an α -solid solution based on *Fe* and oxides FeO , Fe_2O_3 and Fe_3O_4 .

Determination of micromechanical properties of sprayed coatings

Based on the results of instrumental microindentation, it was found that the highest level of microhardness was possessed by the first metal layer (**1**) for coating **A** the microhardness was 1,030 HV 0.1. The first (metal) layer (**1**) in coating **B** was characterized by a microhardness of 745 HV 0.1. The increased hardness of the metal layer of coating **A** is associated with a high content of strengthening phases in it. The microhardness of the transition layer (**2**) is 650 HV 0.1 for coating **A** and 580 HV 0.1 for coating **B**. The microhardness of the outer oxide layer (**3**) for both coatings is 290 HV 0.1. The variation of microhardness in related areas reaches $\sim 350\text{--}380$ HV 0.1 for coating **A** and $\sim 150\text{--}300$ HV 0.1 for coating **B**, which is explained by a decrease in the volume fraction of the strengthening phase (Tables 2 and 4).

The strengthening phases in the coatings reduce the values of maximum and residual indentation depths h_{max} and h_p , which leads to an increase in the values of indentation hardness at maximum load H_{IT} (meaning an increase in resistance to permanent deformation) and Martens hardness HM , which takes into account both plastic and elastic deformation, the indentation elastic modulus E^* of both coatings changes insignificantly (Fig. 4 *a* and 5 *a* in Tables 2 and 4).

In earlier studies [18, 19] it was shown that such parameters as elastic recovery R_e (characterizes the share of elastic deformation in the total deformation during indentation), and indices of the plastic component of work ϕ and creep CIT are used to assess the resistance of surface layers to mechanical action.

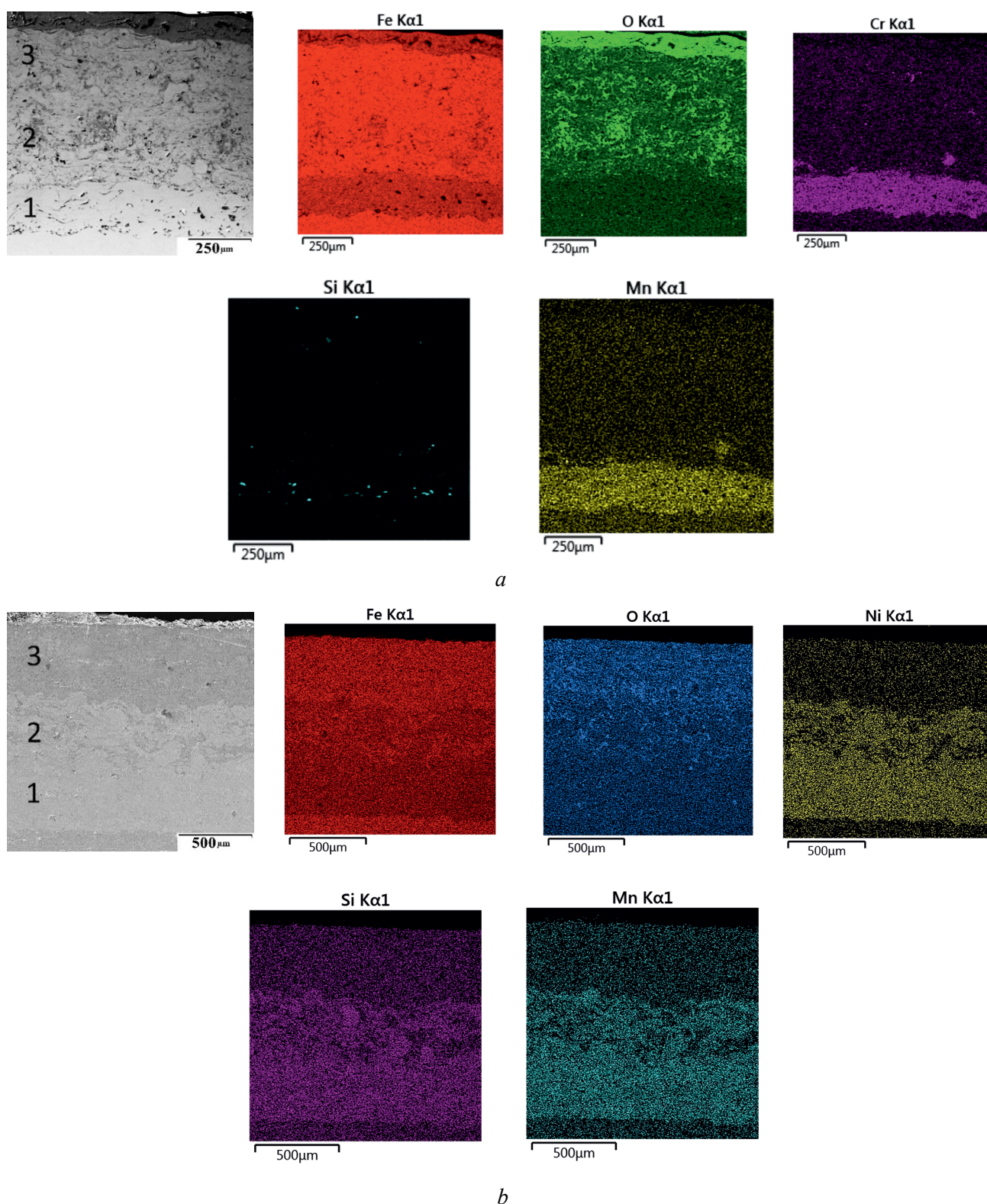


Fig. 3. Microstructure and distribution of elements in the coatings:
a – coating A; b – coating B

As can be seen from Tables 3 and 5 and Figures 4 *b* and 5 *b* in the transition and oxide layer (2) and (3), the creep parameters *CIT* and the plastic component of the work φ have maximum values in contrast to the metallic layer (1) this is explained by the increased plasticity of these layers, the purpose of which is to act as a lubricant under high operating loads. The maximum values of the *Re* index are characterized for the metal layer (1), which indicates the ability of this layer to resist mechanical action without plastic deformation in the elastic region.

Table 2

Results of instrumented microindentation of coating A at a maximum load on the indenter of 980 mN (100 g)

Areas of analysis	HM , GPa (± 34)	H_{IT} , GPa (± 43)	HV (± 41)	E^* , GPa (± 10.7)	h_{max} , μm (± 0.34)	h_p , μm (± 0.31)	h_l , μm (± 0.34)
Metal layer (1)	722.6	1090.0	1030	208.8	2.3	1.5	2.2
Transition layer (2)	500.6	686.7	650	173.7	2.8	1.9	2.6
Oxide layer (3)	258.3	305.7	290	150.5	3.9	3.3	3.6

Table 3

Plasticity parameters for coating A

Areas of analysis	R_e , %	φ , %	CIT , %
Metal layer (1)	35	65	4.5
Transition layer (2)	31	67	6.5
Oxide layer (3)	15	84	8.4

Table 4

Results of instrumented microindentation of coating B at a maximum load on the indenter of 980 mN (100 g)

Areas of analysis	HM , GPa (± 34)	H_{IT} , GPa (± 43)	HV (± 41)	E^* , GPa (± 10.7)	h_{max} , μm (± 0.34)	h_p , μm (± 0.31)	h_l , μm (± 0.34)
Metal layer (1)	579.7	787.6	745	199.0	2.7	1.5	2.4
Transition layer (2)	477.2	616.4	580	164.5	2.9	1.6	2.7
Oxide layer (3)	264.2	306.5	290	140.0	3.9	2.7	3.5

Table 5

Plasticity parameters for coating B

Areas of analysis	R_e , %	φ , %	CIT , %
Metal layer (1)	44	70	6.6
Transition layer (2)	43	73	7.4
Oxide layer (3)	28	81	8.9

Determination of tribological properties under sliding friction conditions

The most important requirement for the coatings analyzed in this work is resistance under wear conditions. Tests under sliding friction conditions made it possible to identify general regularities in the behavior of specimens under external loading and form recommendations for its application in real operating conditions [20–22].

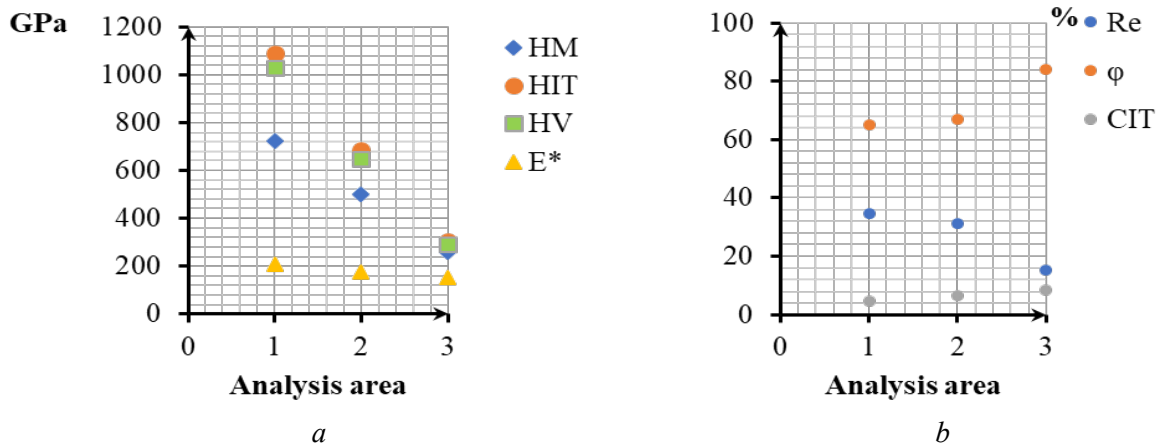


Fig. 4. Average values of strength (a) and ductility (b) of coating **A**:
1 – Oxide layer; 2 – Transition layer; 3 – Metal layer

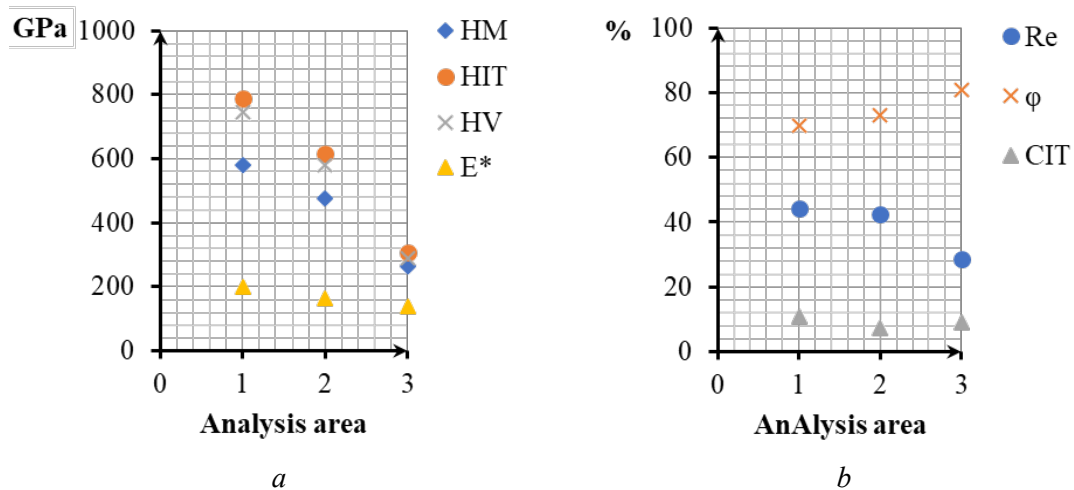


Fig. 5. Average values of strength (a) and ductility (b) of coating **B**:
1 – Oxide layer; 2 – Transition layer; 3 – Metal layer

The results of tribological tests of coatings under sliding friction conditions are presented in Figs. 6 and 7. It is shown that the coating of composition **A** has increased wear resistance compared to the coating of composition **B**, which also agrees with the data obtained on the values of microhardness and micromechanical properties (see Tables 2–5) [23].

Coating **A** is characterized by minimum mass loss (~ 1.5 times less than that of coating **B**) and maximum coefficient of friction ($f \sim 0.3$).

At the initial stage of friction at a load of 30 N there is a run-in period characterized by the highest wear rates (mass loss) and friction coefficients $f \sim 0.6$ for both coatings. Further, at a load of 75 N, the frictional heating temperature of the friction surface increases, which leads to softening of the scale layer and to a decrease in the friction coefficient $f \sim 0.4$ for both coatings, which provides an accelerated transition to steady-state wear.

At a load of 100–130 N, the steady-state wear on the sliding distance is characterized by almost the same change in mass loss (Fig. 6), as well as close levels of friction coefficient $f \sim 0.3$ – 0.4 for coating **A** and $f \sim 0.4$ for coating **B** (Fig. 7). It is worth noting that the temperature of frictional heating of friction surfaces in the case of coating **B** is lower. It is especially noticeable at friction with loads of 30 and 75 N.

The study of wear surfaces of coatings **A** and **B** showed that after sliding friction tests at loads of 30 and 75 N, setting processes characterized by detachment of outer coating particles develop (Fig. 8 a, b and

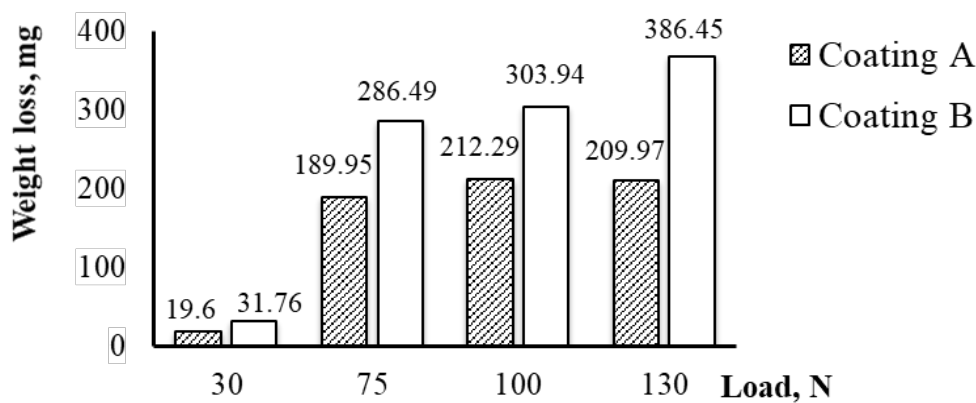
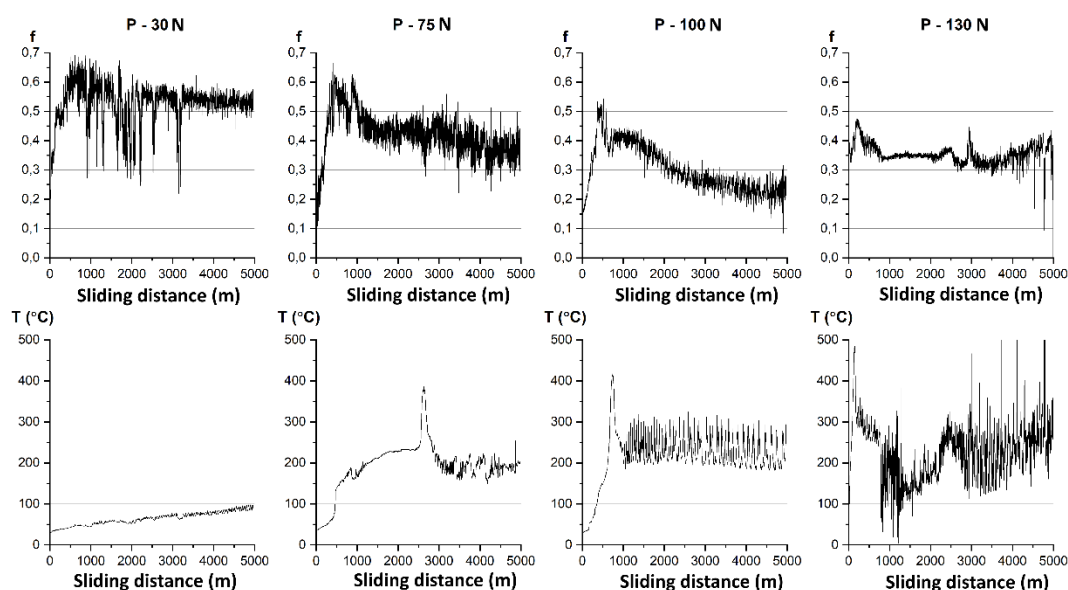
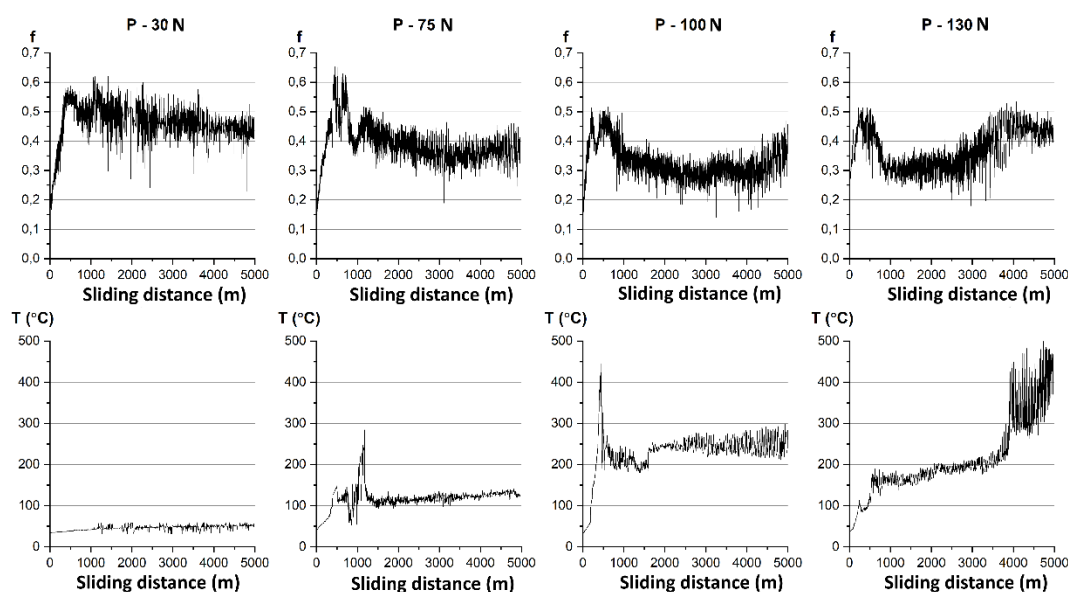


Fig. 6. Weight loss of specimens after testing under sliding friction conditions



a



b

Fig. 7. Friction coefficient f and temperature T (°C) near sliding friction surfaces:

a – coating A; b – coating B

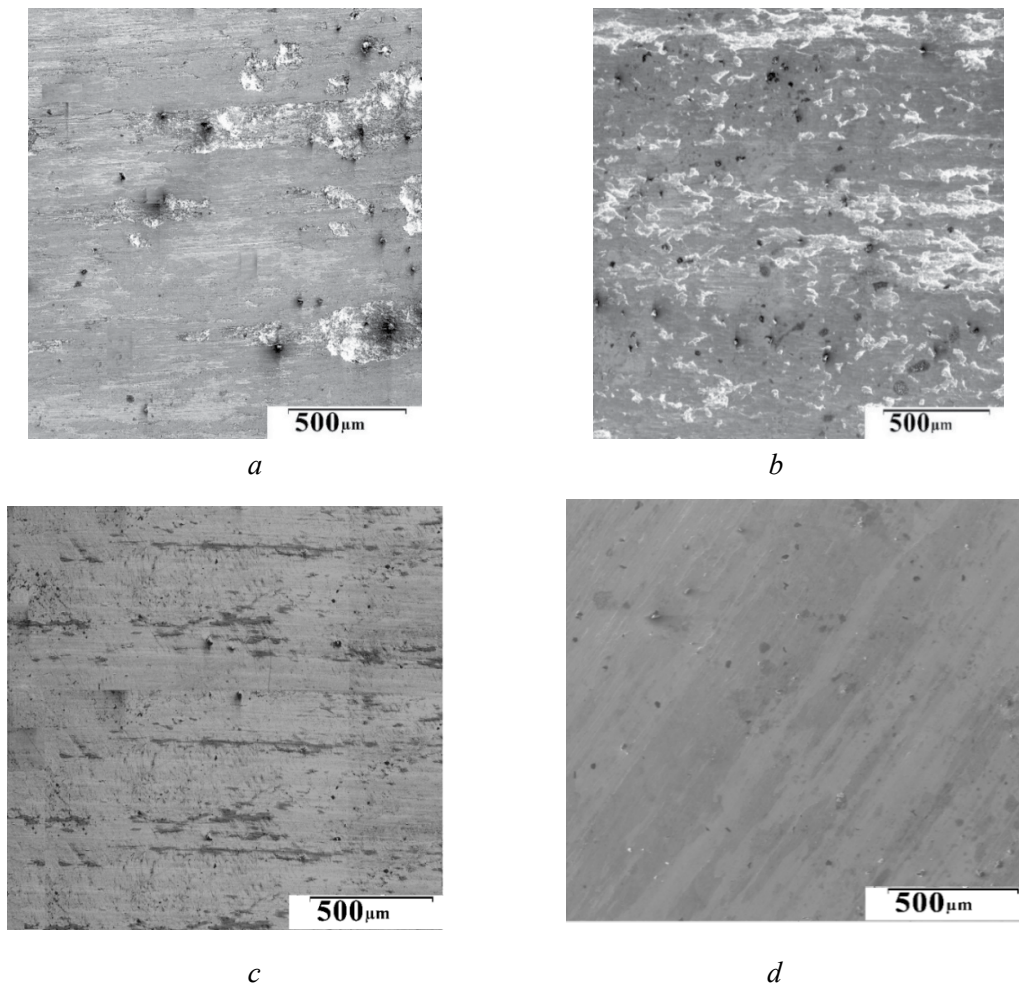


Fig. 8. Coating A surfaces after sliding friction tests:
a – load 30 N; *b* – load 75 N; *c* – load 100 N; *d* – load 130 N

Fig. 9 *a, b*). With increasing load (100 and 130 N), when the oxide layer is almost completely worn out, the metal layer of the coatings of compositions *A* and *B* provides the transition to wear by the mechanism of plastic displacement (Fig. 8 *c, d* and Fig. 9 *c, d*), which corresponds to a decrease in the magnitude of wear.

The study of the chemical composition of the wear surfaces showed that at all selected test loads under sliding friction conditions the inner layers of both compositions were preserved at a maximum load of 130 N (Tables 6 and 7). This confirms the purpose of these layers to prevent tool fracture, which allows timely restoration of wearied outer layers.

The results of studies of surface roughness of coatings *A* and *B* showed that after sliding friction tests there is a smoothing of the initial surface roughness and a decrease in the value of the arithmetic mean deviation of the profile *Ra*. The minimum values of the arithmetic mean deviation of the *Ra* profile are observed after a load of 30 N (*Ra* = 0.434 μm for coating *A* and *Ra* = 0.99 μm for coating *B*), where the wear of the surface oxide layer, which plays the role of lubrication, occurs. As the sliding friction load increases from 75 N to 130 N, the average *Ra* value increases (see Fig. 10 *c–e* and Fig. 11 *c–e*).

Analysis of the surface micro-profile taken during 3D profilometry showed that after friction with 30 and 75 N load, isolated depressions related to the setting processes were observed (Fig. 10 *b, c* and Fig. 11 *b, c* shown by arrows). The surfaces after friction with a load of 100 and 130 N (Fig. 10 *d, e* and Fig. 11 *d, e*) are characterized by the presence of unidirectional protrusions and depressions. Higher values of roughness parameter *Ra* for coating *B* after sliding friction tests are characterized by the presence of more oxides on the surface (see Tables 6 and 7).

As a result of the research, it was found that the tribological properties of the studied coatings depend on the chemical composition of the sprayed material and the resulting strengthening phases.

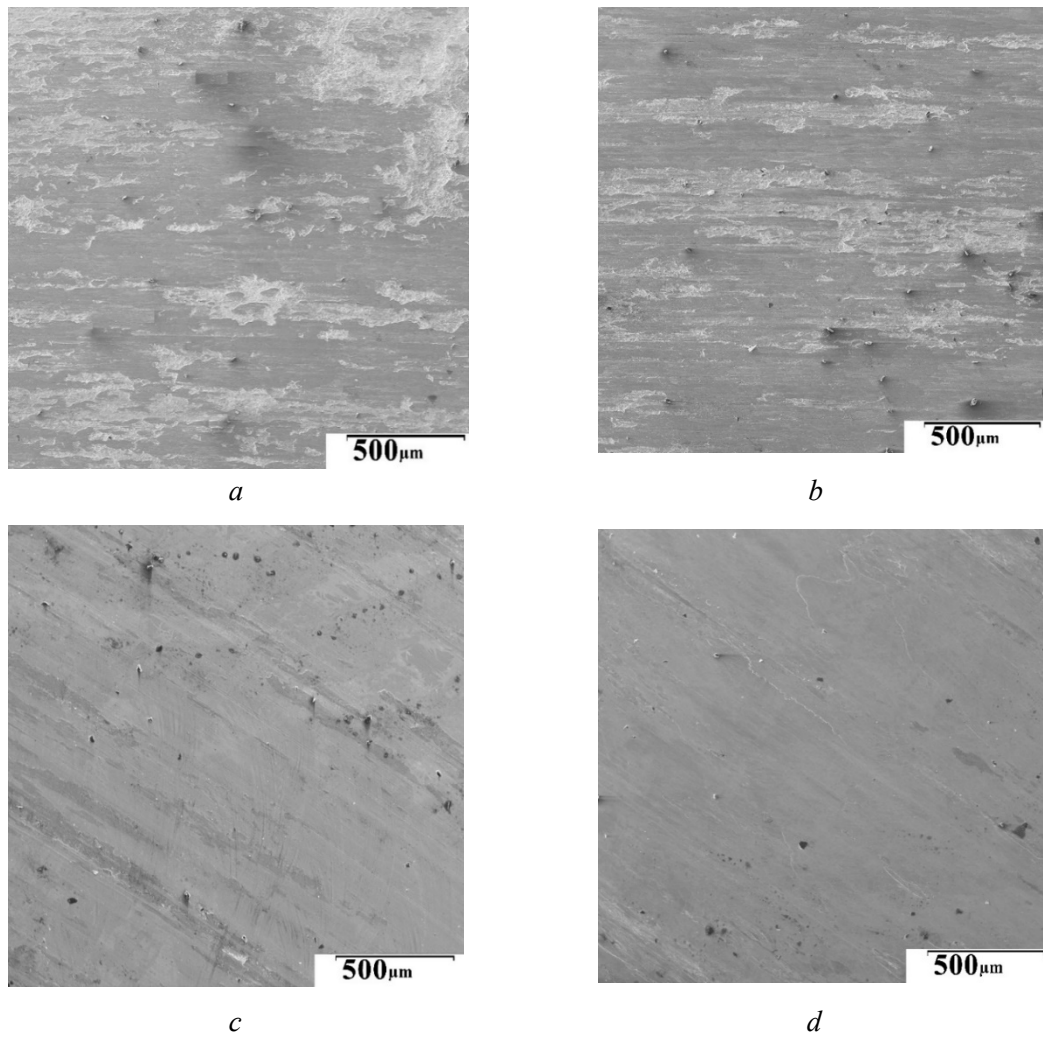


Fig. 9. Coating **B** surfaces after sliding friction tests:
a – load 30 N; *b* – load 75 N; *c* – load 100 N; *d* – load 130 N

Table 6

Chemical composition of the wear surface of the coating *A*, at. %

Load	<i>Fe</i>	<i>O</i>	<i>Cr</i>	<i>Mn</i>	<i>Si</i>	<i>B</i>	<i>C</i>
30 N	56.30	4.87	0.23	0.11	0.14	7.15	4.87
75 N	47.45	4.63	0.72	0.24	0.54	7.41	4.63
100 N	63.03	9.63	2.42	1.15	1.84	11.40	8.00
130 N	57.63	13.23	2.74	1.30	1.87	13.24	6.87

Table 7

Chemical composition of the wear surface of the coating *B*, at. %

Load	<i>Fe</i>	<i>O</i>	<i>Ni</i>	<i>Mn</i>	<i>Si</i>	<i>B</i>	<i>C</i>
30 N	60.59	38.02	0.13	0.20	0.17	0.00	0.00
75 N	61.67	29.34	3.91	1.94	1.47	2.19	1.07
100 N	61.06	28.25	4.80	2.17	1.76	2.46	1.48
130 N	59.36	28.13	6.28	2.28	1.72	4.07	1.00

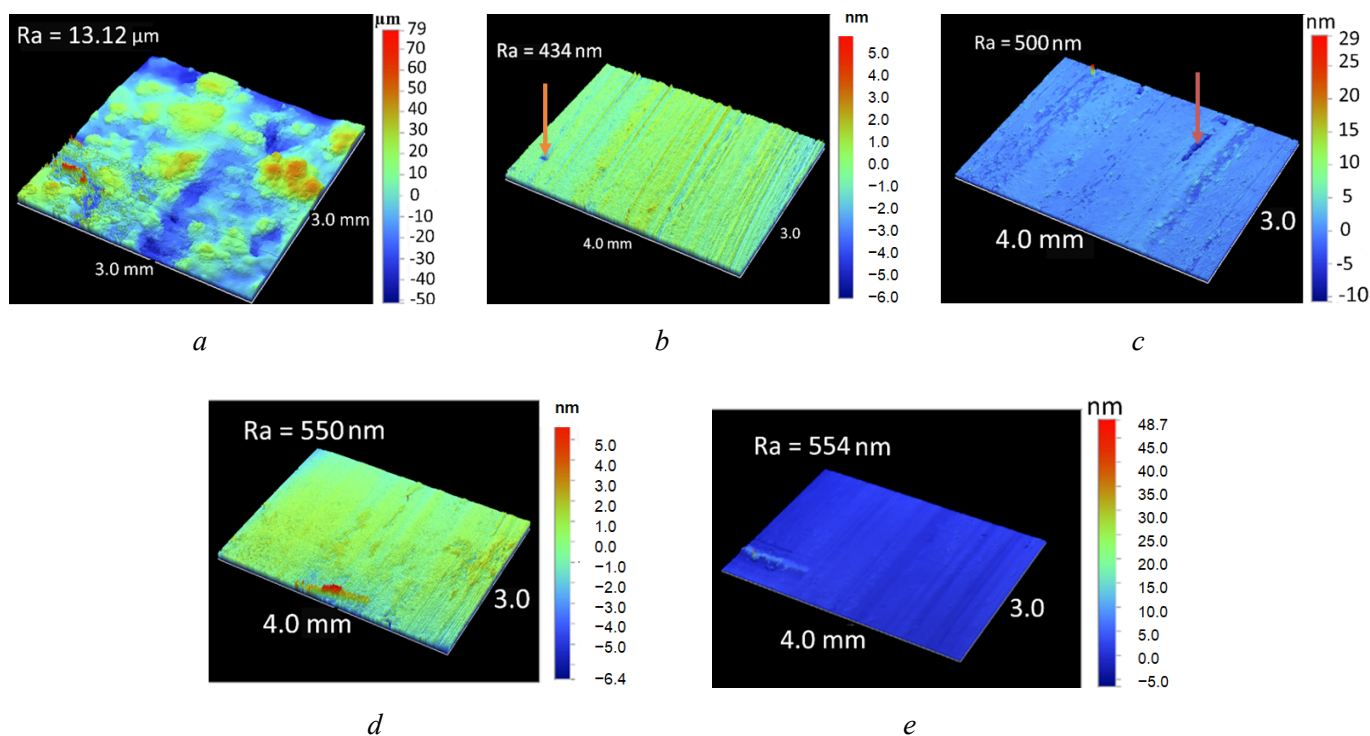


Fig. 10. 3-D profilograms of the coated specimen **A**:

a – in the initial state; *b* – after a wear test at a load of 30 N; *c* – 75 N; *d* – 100 N; *e* – 130 N

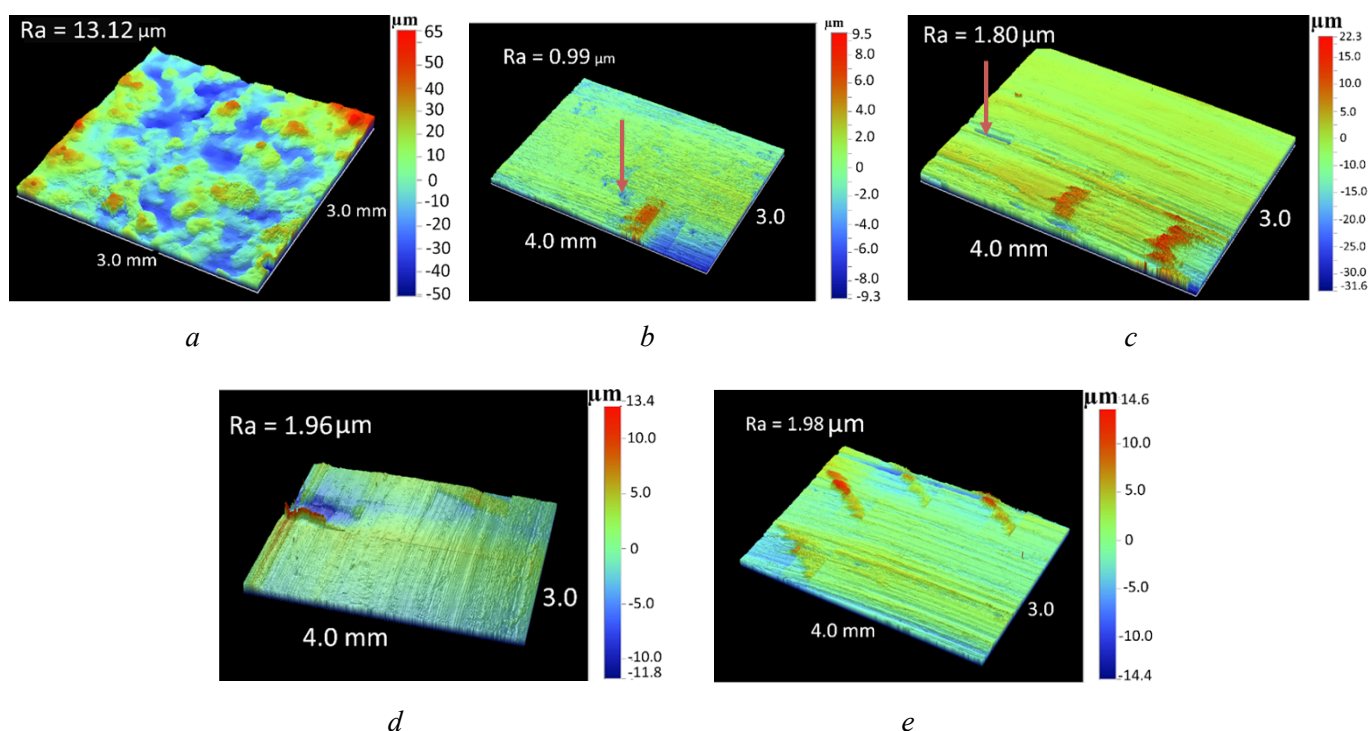


Fig. 11. 3-D profilograms of the coated specimen **B**:

a – in the initial state; *b* – after a wear test at a load of 30 N; *c* – 75 N; *d* – 100 N; *e* – 130 N

The strengthening phases formed in the process of plasma spraying contribute to an increase in the microhardness and wear resistance of the materials under study, as well as a decrease in the intensity of wear under conditions of dry sliding friction.

Conclusion

High-temperature coatings obtained by plasma spraying consist of successively applied layers: the first inner (metal) layer is obtained by spraying self-fluxing powders of two different compositions of *Fe-Cr-Si-Mn-B-C* system (composition **1**) and *Fe-Ni-Si-Mn-B-C* system (composition **2**); the second layer is a transitional layer obtained by spraying a mixture of high-temperature powders of compositions **1** or **2**, with *Fe* powder in the ratio of 50:50 and the outer (metal-oxide) layer is obtained by spraying *Fe* powder in an oxidizing atmosphere to form an oxide layer consisting of a mixture of iron oxides ($FeO + Fe_2O_3 + Fe_3O_4$) on the surface. The total thickness of the obtained coatings is 800–850 μm .

The inner (metal) layer is characterized by high hardness (up to 1,030 HV 0.1 for coating composition **1** and 745 HV 0.1 for coating composition **2**) and *Re* values, which indicates the ability of this layer to resist mechanical stress without plastic deformation in the elastic region.

High plasticity indices of outer layers (creep *CIT* and plastic component of work ϕ) are established, the purpose of which is to act as a lubricant under high operating loads.

Under conditions of dry sliding friction, it is shown that coating *A* has increased wear resistance compared to coating *B*; the friction coefficient for coating *A* is $f = 0.3$, the friction coefficient for coating *B* is $f = 0.4$.

The study of the wear surfaces showed that on the surface of the obtained coatings after sliding friction tests at the load of 30 and 75 N the processes of seizure develop, and at increasing the load to 100 N and 130 N there is a transition to wear by the mechanism of plastic displacement, which corresponds to a decrease in the magnitude of wear. Under all selected test loads under conditions of dry sliding friction, high-temperature layers of coatings of both compositions are preserved at the maximum load of 130 N. After the sliding friction tests, a significant surface smoothing and a reduction in the arithmetic mean deviation of the *Ra* profile are recorded.

References

1. Guzanov B.N., Kositsyn S.V., Pugacheva N.B. *Uprochnyayushchie zashchitnye pokrytiya v mashinostroenii* [Reinforcing protective coatings in engineering industry]. Ekaterinburg, UrO RAN Publ., 2003. 244 p. ISBN 5-7691-1405-3.
2. Serin K., Pehle H.J. Improved service life for hot forming tools in seamless tube plants. *Stahl und Eisen*, 2014, vol. 134 (11), pp. 161–174.
3. Sivakumar R., Mordike B.L. High temperature coatings for gas turbine blades: a review. *Surface and Coatings Technology*, 1989, vol. 37 (2), pp. 139–160. DOI: 10.1016/0257-8972(89)90099-6.
4. Podshivalkin S.A., Torbeev A.N. Struktura i svoystva oksidirovannykh pokrytii [Structure and properties of oxidized coatings]. *Master's Journal*, 2012, no. 2, pp. 91–98. (In Russian).
5. Fomin A.A., Steinhauer A.B., Lyasnikov V.N., Wenig S.B., Zakharevich A.M. Nanocrystalline structure of the surface layer of plasma-sprayed hydroxyapatite coatings obtained upon preliminary induction heat treatment of metal base. *Technical Physics Letters*, 2012, vol. 38 (5), pp. 481–483. DOI: 10.1134/S1063785012050227.
6. Sazonenko I.O., Zemuov V.A., Yurchak A.N. K voprosu povysheniya stoikosti opravok proshivnykh stanov [To the matter of stabilization of saddles of punch mills]. *Lit'e i metallurgiya = Foundry Production and Metallurgy*, 2012, no. 4, pp. 135–138. (In Russian).
7. Pukhov E.V., Zagoruyko K.V. Rezul'taty eksperimental'nykh issledovaniy iznosostoikosti poverkhnosti kolenchatogo vala, vosstanovlennoi metodom gazoplamennogo naneseniya samoflyusuyushchikhsya poroshkov [The results of experimental studies of the wear resistance of the surface of the crankshaft restored by the method of flame application of self-fluxing powders]. *Mezhdunarodnyi tekhniko-ekonomicheskii zhurnal = The International Technical-Economic Journal*, 2020, no. 4, pp. 45–52. DOI: 10.34286/1995-4646-2020-73-4-45-52. (In Russian).
8. Manoilo E.D., Radchenko A.A., Shardakov S.N. [Continuous gas-flame coating of self-fluxing alloy powders on rod couplings of oil pumps]. *Poroshkovaya metallurgiya: inzheneriya poverkhnosti, novye poroshkovye kompozitsionnye materialy. Svarka* [Powder metallurgy: surface engineering, new powder composite materials. Welding]. Collection of reports of the 13th International Symposium. Pt. 2. Minsk, 2023, pp. 171–186. (In Russian).



9. Budinovskiy S.A., Muboyadzhyan S.A., Gayamov A.M., Matveev P.V. Development of ion-plasma refractory metallic layers of heat-insulating coatings for cooled turbine rotor blades. *Metal Science and Heat Treatment*, 2014, vol. 55, pp. 652–657. DOI: 10.1007/s11041-014-9684-2.

10. Krivonosova E., Gorchakov A. Micro-arc oxidation as efficient technology of increasing of wear resistance of aluminum alloy. *Elektrotehnika & Elektronika E+E*, 2013, vol. 48 (5–6), pp. 352–355.

11. Iida S., Hidaka Y. Influence of iron oxide of carbon steel on lubricating properties in seamless pipe hot rolling and the effectiveness of borax application. *Tetsu-to-Hagane / Journal of the Iron and Steel Institute of Japan*, 2010, vol. 96 (9), pp. 550–556. DOI: 10.2355/tetsutohagane.96.550.

12. Rodionov I.V. Application of the air-thermal oxidation technology for producing biocompatible oxide coatings on periosteal osteofixation devices from stainless steel. *Inorganic Materials: Applied Research*, 2013, vol. 4 (2), pp. 119–126. DOI: 10.1134/S2075113313020159.

13. Wang Y., Liu Y., Tang H., Li W., Han C. Oxidation behavior and mechanism of porous nickel-based alloy between 850 and 1000 °C. *Transactions of Nonferrous Metals Society of China*, 2017, vol. 27 (7), pp. 1558–1568. DOI: 10.1016/S1003-6326(17)60177-8.

14. Mar'in D.M., Glushchenko A.A., Salakhutdinov I.R. Snizhenie iznosa porshnei dvigatelya vnutrennego sgoraniya oksidirovaniem rabochikh poverkhnostei golovok [Reduced wear of pistons of internal combustion engine by oxidation of the working surfaces of the heads]. *Transport. Transportnye sooruzheniya. Ekologiya = Transport. Transport facilities. Ecology*, 2018, no. 2, pp. 71–79. DOI: 10.15593/24111678/2018.02.08.

15. Gerasimov Yu.L., Avdeev S.V., Bobarikin Yu.L. Issledovanie vliyaniya osobennostei oksidirovannogo pokrytiya proshivnykh opravok na ikh ekspluatatsionnyuyu stoikost' [Study of the influence of the features of the oxidized coating of piercing mandrels on their operational durability]. *Chernye metally = Stahl und Eisen*, 2017, no. 7, pp. 46–49. (In Russian).

16. Oliver W.C., Pharr J.M. An improved technique for determining hardness and elastic modulus using load and displacement sensing indentation experiments. *Journal of Materials Research*, 1992, vol. 7 (6), pp. 1564–1583. DOI: 10.1557/JMR.1992.1564.

17. Pugacheva N.B., Nikolin Yu.V., Bykova T.M., Goruleva L.S. Chemical composition, structure and microhardness of multilayer high-temperature coatings. *Obrabotka metallov (tekhnologiya, oborudovanie, instrumenty) = Metal Working and Material Science*, 2022, vol. 24, no. 4, pp. 138–150. DOI: 10.17212/1994-6309-2022-24.4-138-150. (In Russian).

18. Cheng Y.T., Cheng C.M. Relationships between hardness, elastic modulus and the work of indentation. *Applied Physics Letters*, 1998, vol. 73 (5), pp. 614–618. DOI: 10.1063/1.121873.

19. Page T.F., Hainsworth S.V. Using nanoindentation techniques for the characterization of coated systems: a critique. *Surface and Coatings Technology*, 1993, vol. 61 (1–3), pp. 201–208. DOI: 10.1016/0257-8972(93)90226-E.

20. Guzanov B.N., Pugacheva N.B., Bykova T.M. Corrosion and erosion resistance of the combined multilayer coating for the protection of critical parts of modern gas turbine engines. *Diagnostics, Resource and Mechanics of Materials and Structures*, 2021, iss. 2, pp. 6–21. DOI: 10.17804/2410-9908.2021.2.006-021. (In Russian).

21. Guzanov B.N., Obabkov N.V., Migacheva G.N. Development and research of multi-layer composite coatings high temperature. *Sciences of Europe*, 2017, no. 16-1 (16), pp. 83–88. (In Russian).

22. Sivakumar R., Mordike B.L. High temperature coatings for gas turbine blades: a review. *Surface and Coatings Technology*, 1989, vol. 37 (2), pp. 139–160. DOI: 10.1016/0257-8972(89)90099-6.

23. Makarov A.V., Skorynina P.A., Osintseva A.L., Yurovskikh A.S., Savray R.A. Improving the tribological properties of austenitic 12Kh18N10T steel by nanostructuring frictional treatment. *Obrabotka metallov (tekhnologiya, oborudovanie, instrumenty) = Metal Working and Material Science*, 2015, no. 4 (69), pp. 80–92. DOI: 10.17212/1994-6309-2015-4-80-92. (In Russian).

Conflicts of Interest

The authors declare no conflict of interest.

